Numerical validation of a synthetic cell-based model of blood coagulation

Jevgenija Pavlova[1], Antonio Fasano[2,3,4], João Janela[5], and Adélia Sequeira[1,6]

[1]*CEMAT, IST, Universidade de Lisboa, Portugal*
[2]*Professor Emeritus, Dipartimento di Matematica, "U. Dini", Università degli studi di Firenze, Italy*
[3]*Scientific Manager at FIAB SpA, Firenze, Italy*
[4]*Istituto di Analisi dei Sistemi ed Informatica (IASI) Antonio Ruberti, CNR, Italy*
[5]*Departamento de Matemática and CEMAPRE, ISEG, Universidade de Lisboa, Portugal*
[6]*Departamento de Matemática, IST, Universidade de Lisboa, Portugal*

Abstract

In [8] a new reduced mathematical model for blood coagulation was proposed, incorporating biochemical and mechanical actions of blood flow and including platelets activity. The model was characterized by a considerable simplification of the differential system associated to the biochemical network and it incorporated the role of blood slip at the vessel wall as an extra source of activated platelets.

The purpose of this work is to check the validity of the reduced mathematical model, using as a benchmark the model presented in [1], and to investigate the importance of the blood slip velocity in the blood coagulation process.

Keywords: blood coagulation, platelets, biochemical reactions, mathematical modeling, slip boundary conditions, reaction-advection-diffusion equations

1 Introduction

Blood coagulation is an extremely complex biological process in which blood forms clots to prevent bleeding, followed by their dissolution and, on a longer time scale, by repair of the injured tissue. The process involves different interactions between the blood components and the vessel walls. The biological model used nowadays is the so-called cell-based model [5, 13, 14] which during the last decade has replaced the so-called cascade model. According to it the coagulation process is subdivided into five phases: initiation, amplification, propagation, termination and fibrinolysis. Each phase develops through a biochemical network including positive and negative feedback mechanisms. A failure at any stage of the process leads to bleeding or thrombotic disorders.

Due to the complexity of the biochemical network, constantly interacting with the blood flow and dependent on platelets activity, mathematical modeling and numerical implementation offer serious difficulties. The literature on mathematical models for blood coagulation has grown at an impressive pace during the last years (see [2, 3, 4, 7, 10, 17, 19, 24, 25] and the review [9]).

In our previous work [8] a synthetic model for blood coagulation was proposed. This model studies the clot evolution and its subsequent dissolution combining the action of the blood flow with cellular and molecular processes, and possessing some novelties.

In particular, a coefficient was introduced weighing the contribution of activated platelets, which is obviously a fundamental aspect in the process. Such a coefficient enters as a factor of the reaction rate for the prothrombinase production that implicitly affects all other platelets-mediated chemical reactions, such as those involving prothrombin, thrombin, fibrin, etc. Actu-

ally, the amount of the coagulation factors produced and consumed during the clot formation is strongly dependent on the concentration of activated platelets at the injury site, though such a circumstance is frequently ignored in mathematical models.

We also consider the possibility that an additional source of activated platelets at the clotting site may be provided by the blood slip velocity. Therefore, in our view the progressing clot front is capturing not only the platelets being on its way, but also those carried to the clotting site by the slipping flow. Such a mechanism is likely to contribute much more than e.g. diffusion. That provides an explanation of the phenomenon that in different blood vessels, such as veins and arteries, different blood clots structures are observed [11]. Let us point out that slip at the vessel wall, though normally disregarded, is a rather natural phenomenon for blood, due to its composite structure. It is well known that a thin erythrocytes free layer is present at the wall (to which a no-slip condition can be imposed), but when treating blood as a homogeneous fluid one must take into account that cells have a finite velocity very close to the wall and this condition is conveniently described as slip.

The simplification of the differential system describing the biochemical cascade reduces model complexity by a large extent. This is particularly important in view of the coupling with a difficult flow problem in variable geometry.

Our main concern was to focus on the propagation phase of blood coagulation, when the main portion of thrombin is formed. Thus we omit the initial and amplification phases (that in terms of time scales are much shorter), starting after the so called primary coagulation (platelet driven) and from the moment when a small amount of thrombin and of other acti-

vated factors has been already formed.

As a benchmark for our computations the mathematical model proposed in [1] has been chosen, describing the blood coagulation process from the early stage till the complete blood clot dissolution and combining the biochemistry with the blood flow dynamics. The biochemical differential system in [1] includes 23 chemical reactions corresponding to the five blood coagulation phases.

According to the reduced model here adopted ten equations of the benchmark model were replaced by only one virtual equation for prothrombinase production that stands as an output of the amplification phase. Such an approach makes sense only if one is not interested in the evolution of the factors that are omitted, thus the reduced model is not adequate to study the disorders associated to the deficiency or dysfunction of those factors.

Comparison with the benchmark model allows to provide the missing data for the reduced model, with particular reference to the rate constants appearing in the virtual equation for prothrombinase. Owing to the extremely demanding computational complexity, numerical simulations have been performed in a one-dimensional case.

In consideration of the limited purposes of this first step, we took diffusion as the only transport mechanism, necessarily omitting the action of the blood flow. As a consequence, the contribution of the slipping flow is likewise disregarded, consistently with the fact that the role of platelets is not explicitly included in the benchmark model [1].

Once the synthetic model has been suitably tuned, numerical simulations are performed in the two-dimensional case, adding the action of the blood flow and blood slip velocity. To show the impact of the latter quantity on the evolution of biochemical reactions, these results are compared with the no-

slip velocity case, in which the activated platelets concentration is constant.

The outline of the paper is the following. In Section 2 we briefly describe the synthetic and the benchmark models for the blood coagulation process; in Section 3 we give the numerical resolution of the benchmark and synthetic models in the one-dimensional case and provide the initial conditions and unknown parameters for the virtual equation; in Section 4 we show the numerical results in the two-dimensional case considering the impact of the blood slip velocity on the propagation of chemical reactions and compare them with no-slip velocity case. The paper ends with conclusions and some perspectives of future work.

2 Mathematical models for blood coagulation

We start this section by presenting a system of equations that describes two mathematical models for blood coagulation, namely the benchmark and the synthetic models.

We consider an initial-boundary value problem composed of n ($n = 13$ in the case of the synthetic model and $n = 23$ for the benchmark model) time dependent reaction-advection-diffusion (RAD) equations, mutually coupled through linear and non-linear reaction terms. The system is complemented by initial conditions and (non-)homogeneous Neumann boundary conditions B_i, $i = 1, \ldots, n$ providing input fluxes at the boundary $\partial\Omega$ of the injury site, see Table 1

$$\begin{cases} \frac{\partial [C_i]}{\partial t} = \operatorname{div}(D_i \nabla [C_i]) + R_i - \operatorname{div}(\mathbf{u} \cdot [C_i]), & \text{in } Q_T := (0,T) \times \Omega, \\ D_i \frac{\partial [C_i]}{\partial \mathbf{n}} = B_i, & \text{on } \Sigma_T := (0,T) \times \partial\Omega, \\ [C_i] = [C_i]^{blood}, & \text{for } t = 0. \end{cases} \quad (1)$$

Here, $[C_i]$ is the unknown function that describes the evolution of concentration of the coagulation factors in time in the domain Ω, R_i are the reaction terms that depend on the evolution of concentrations $[C_i]$, D_i are diffusion coefficients, $\mathbf{u}$ is the blood flow velocity and $[C_i]^{blood}$ are the initial concentrations.

The authors of [1] provide a complete list of the required biochemical parameters collected through various laboratory experiments.

In the next section we list the reaction terms for both models and briefly explain the biological meaning of the considered biochemical reactions.

2.1 Benchmark model

The biochemical network of the benchmark model [1] is reported below. The corresponding reaction rates are listed in Table 2[1]:

$$R_{XIa} = \frac{k_{11}[IIa][XI]}{K_{11M} + [XI]} - h_{11}^{A3}[XIa][ATIII] - h_{11}^{L1}[XIa][\alpha_1 AT], \quad (2)$$

$$R_{XI} = -\frac{k_{11}[IIa][XI]}{K_{11M} + [XI]}, \quad (3)$$

$$R_{IXa} = \frac{k_9[XIa][IX]}{K_{9M} + [IX]} - h_9[IXa][ATIII], \quad (4)$$

$$R_{IX} = -\frac{k_9[XIa][IX]}{K_{9M} + [IX]}, \quad (5)$$

$$R_{Xa} = \frac{k_{10}[Z][X]}{K_{10M} + [X]} - h_{10}[Xa][ATIII] - h_{TFPI}[TFPI][Xa], \quad (6)$$

$$R_X = -\frac{k_{10}[Z][X]}{K_{10M} + [X]}, \quad (7)$$

$$R_{VIIIa} = \frac{k_8[IIa][VIII]}{K_{8M} + [VIII]} - h_8[VIIIa] - h_{C8}\frac{[APC][VIIIa]}{H_{C8M} + [VIIIa]}, \quad (8)$$

$$R_{VIII} = -\frac{k_8[IIa][VIII]}{K_{8M} + [VIII]}, \quad (9)$$

[1]Notation [F] denotes the concentration of the coagulation factor F.

$$R_{Va} = \frac{k_5[IIa][V]}{K_{5M} + [V]} - h_5[Va] - h_{C5}\frac{[APC][Va]}{H_{C5M} + [Va]}, \tag{10}$$

$$R_V = -\frac{k_5[IIa][V]}{K_{5M} + [V]}, \tag{11}$$

$$[Z] = \frac{[VIIIa][IXa]}{K_{dZ}}, \tag{12}$$

$$[W] = \frac{[Va][Xa]}{K_{dW}}, \tag{13}$$

$$R_{IIa} = \frac{k_2[W][II]}{K_{2M} + [II]} - h_2[IIa][ATIII], \tag{14}$$

$$R_{II} = -\frac{k_2[W][II]}{K_{2M} + [II]}, \tag{15}$$

$$R_{Ia} = \frac{k_1[IIa][I]}{K_{1M} + [I]} - \frac{h_1[PLA][Ia]}{H_{1M} + [Ia]}, \tag{16}$$

$$R_I = -\frac{k_1[IIa][I]}{K_{1M} + [I]}, \tag{17}$$

$$R_{ATIII} = -h_9[IXa][ATIII] - h_{10}[Xa][ATIII] - \tag{18}$$
$$- h_2[IIa][ATIII] - h_{11}^{A3}[XIa][ATIII],$$

$$R_{APC} = \frac{k_{PC}[IIa][PC]}{K_{PCM} + [PC]} - h_{PC}[APC][\alpha_1 AT], \tag{19}$$

$$R_{PC} = -\frac{k_{PC}[IIa][PC]}{K_{PCM} + [PC]}, \tag{20}$$

$$R_{\alpha_1 AT} = -h_{PC}[APC][\alpha_1 AT] - h_{11}^{A3}[XIa][ATIII], \tag{21}$$

$$R_{TFPI} = -h_{TFPI}[TFPI][Xa], \tag{22}$$

$$R_{tPA} = 0, \tag{23}$$

$$R_{PLA} = \frac{k_{PLA}[tPA][PLS]}{K_{PLAM} + [PLS]} - h_{PLA}[PLA][\alpha_2 AP], \tag{24}$$

$$R_{PLS} = -\frac{k_{PLA}[tPA][PLS]}{K_{PLAM} + [PLS]}, \tag{25}$$

$$R_{\alpha_2 AP} = -h_{PLA}[PLA][\alpha_2 AP]. \tag{26}$$

All these reaction terms describe the generation and depletion of active

and non-active coagulation and fibrinolysis factors that follow first-order, second-order or Michaelis-Menten kinetics. We refer to [1] for the meaning of symbols (which are well known in the coagulation context) in order to save space. We just recall that W stands for prothrombinase and Z for tenase.

The following phases can be distinguished in this mathematical model: initiation, resulting in the production of small amounts of factors IXa, Xa and XIa triggered by the boundary conditions given in Table 1; amplification, with the consequent activation of factors V, VIII, IX, X and XI (described by equations (2)–(11)) leading to the production of the tenase and prothrombinase complexes (equations (12) and (13)), in turn responsible for the thrombin burst, marking the beginning of the propagation phase (equations (14)–(20)) when the main portion of fibrin is produced. The inhibitors ATIII, APC, α_1AT and TFPI keep under control the production of coagulation factors and eventually lead to the termination phase. The chain of chemical reactions ends with the fibrinolysis process resulting in plasmin production that will finally dissolve the fibrin clot (equations (21)–(26)).

2.2 Synthetic model

We recall that the synthetic model captures the propagation, termination and fibrinolysis phases and focusses on the production of platelets mediated coagulation factors, such as prothrombinase, thrombin and fibrin. The intermediate cascade section involving factors V, VIII, IX, X, XI and the tenase compex Z, corresponding to equations (2)–(12) in the benchmark model is replaced by one equation for the prothrombinase production (27). This equation includes the possible effect of blood slip velocity which may provide an extra supply of activated platelets at the clotting region, resulting in a higher thrombin production.

Below we list the set of reaction rates for the synthetic blood coagulation model

$$R_W = k_W C_P [IIa] \left(1 - \frac{[IIa]}{[IIa]^*}\right) - \left(h_{1W}[APC] + h_{2W}[ATIII]\right)[W], \tag{27}$$

$$R_{IIa} = \frac{k_2[W][II]}{K_{2M} + [II]} - h_2[IIa][ATIII], \tag{28}$$

$$R_{II} = -\frac{k_2[W][II]}{K_{2M} + [II]}, \tag{29}$$

$$R_{Ia} = \frac{k_1[IIa][I]}{K_{1M} + [I]} - \frac{h_1[PLA][Ia]}{H_{1M} + [Ia]}, \tag{30}$$

$$R_I = -\frac{k_1[IIa][I]}{K_{1M} + [I]}, \tag{31}$$

$$R_{ATIII} = -h_2[IIa][ATIII] - h_{2W}[W][ATIII], \tag{32}$$

$$R_{APC} = \frac{k_{PC}[IIa][PC]}{K_{PCM} + [PC]} - h_{PC}[APC][\alpha_1 AT] - h_{1W}[APC][W], \tag{33}$$

$$R_{PC} = -\frac{k_{PC}[IIa][PC]}{K_{PCM} + [PC]}, \tag{34}$$

$$R_{\alpha_1 AT} = -h_{PC}[APC][\alpha_1 AT], \tag{35}$$

$$R_{tPA} = 0, \tag{36}$$

$$R_{PLA} = \frac{k_{PLA}[tPA][PLS]}{K_{PLAM} + [PLS]} - h_{PLA}[PLA][\alpha_2 AP], \tag{37}$$

$$R_{PLS} = -\frac{k_{PLA}[tPA][PLS]}{K_{PLAM} + [PLS]}, \tag{38}$$

$$R_{\alpha_2 AP} = -h_{PLA}[PLA][\alpha_2 AP]. \tag{39}$$

As in the benchmark model we may recognize the chemical reactions corresponding to the propagation, termination and fibrinolysis phases. Equations (27)–(31) refer to the propagation phase, initially assuming that a small blood clot that covers the injury site has been already formed. In this setting,

the process starts from the prothrombinase activation by thrombin described by the virtual equation (27). At the same time prothrombinase production is regulated by the inhibitors, namely activated protein C and antithrombin III, present in the circulating blood. We stress the fact that the reactions described in (27) do not take place in reality: they just describe a shortcut to represent the indirect influence of APC and ATIII on prothrombinase production, whose real path is actually more complicated, as shown in the benchmark model.

The factor C_P in this equation represents the dimensionless activated platelets concentration defined as the ratio between the actual and the standard platelets concentration in blood. The definition proposed is[2]

$$C_P = \left(1 + \frac{1}{2}\frac{A_P}{V_n}\frac{h}{H}u_s\frac{[Ia]}{[Ia]^*}\frac{u}{u_s}\right). \tag{40}$$

Here, the factor $\frac{1}{2}$ stands as an assumption that the slip velocity occurs mainly upstream the clot; $H = \frac{\sigma}{L_\Omega}$ is a length depending on the injury shape and its orientation towards the blood flow (σ = area of the lesion, L_Ω = projection of the lesion diameter transverse to the flow), and u_s is the blood slip velocity[3]. Moreover, $[IIa]^*$ in (27) represents the maximum expected thrombin concentration and k_W, h_{1W} and h_{2W} are the prothrombinase production and inhibition rates, given in Table 2 (these coefficients have no direct biological meaning, since they are not related to real chemical reactions and have been deduced by comparison with the benchmark model).

The cascade proceeds with the activation of prothrombin by prothrombinase. Then prothrombinase proteolytically cleaving it to form thrombin. Thrombin converts soluble fibrinogen to fibrous fibrin. The latter is pro-

[2]We refer to [8] for a full description of C_P.

[3]More details about the model, including the virtual equation and possible extensions may be found in [8, 21, 22].

gressively eliminated (at a slower rate) by plasmin that is formed when plasminogen (constantly present in circulating blood) is activated by tPA released from the endothelial cells. The reaction rates and kinetic constants in (28)–(39) are taken from [1] and listed in Table 2.

3 Numerical resolution

In this section the testing procedure of the synthetic model is discussed and the initial conditions and the unknown parameters for the virtual equation (27) are derived. This will require to solve the benchmark model first. Since the benchmark model does not consider the role of platelets, nor of the possible blood slip velocity, in this phase we omit the fluid dynamics altogether.

We note that the benchmark model was already solved numerically in [6] using the finite volume method. However, the solution of this biochemical system is hard to generalize for all blood vessel types due to its dependence on the blood flow characteristics. Actually, our purpose is not to repeat these calculations, but to select the parameters in equation (27) of the synthetic model and to derive appropriate initial conditions for the reduced model.

While the numerical results of the benchmark model presented in [6] predict the peak of thrombin concentration to appear in approximately 40 seconds after injury, the data available in the literature reports the thrombin peak to occur much later. Therefore, to be closer to the experimental results we have considered a longer thrombin time. For this purpose, the boundary fluxes B_i were downregulated by decreasing the value L, see Table 1. This parameter represents the thickness of the plasma layer above the thrombogenic plane which in [1] has been set equal to 0.2 cm. After several numerical tests evaluating its impact on the whole system, we found that taking it equal to 0.00015 cm the duration of the initial and the amplifi-

cation phases is extended to 1.91 minute obtaining the same concentration peaks of coagulation factors as in [6]. Thus we believe that this choice is more appropriate.

In order to reduce the computational complexity, in our simulations we consider the following computational domains: in a two-dimensional geometry

$$\Omega_{2D} = \{(x_1, x_2) \in \mathbb{R}^2 : -r \leq x_1 \leq r, l_1 \leq x_2 \leq l_2\},$$

and in a one-dimensional geometry

$$\Omega_{1D} = \{x \in \mathbb{R} : -r \leq x \leq r\}.$$

The domains are meant to mimic an "arteriola" of radius r and length $l := l_2 - l_1$. In our case we take $r = 250$ μm, and $l = 1500$ μm.

3.1 Resolution of the benchmark model

We consider the initial boundary value problem, described in [1], that represents the blood coagulation problem modeled according to the intrinsic pathway. The biochemical network of 23 species is considered to form the blood clot which represents the polymer fibrin network entrapping different blood ingredients flowing through it. The system consists of equations (2)–(26), complemented by (non-)homogeneous Neumann boundary conditions B_i, see Table 1. The initial conditions C_i^{blood} are taken from [1] and they correspond to the concentrations of coagulation factors in the circulating blood.

To solve the full problem (1) a first order-operator splitting method (Lie-Trotter splitting) is used [18, 15, 23, 26, 27]. In particular, the differential operators of the main problem are split into two subproblems: the diffusion

and reaction parts that are coupled to each other through the initial conditions. These two subproblems (diffusion and reaction) are solved sequentially on the time interval $[t^0, t^N]$, where $t^0 = 0$ corresponds to the injury moment and $t^N = T$ to the moment when the blood clot is completely dissolved; in our case that corresponds to 30 minutes.

In the case of linear reactions (neglecting the time integration schemes) the error associated to the splitting procedure was proved to be equal to zero [16, 22]. On the contrary, errors may be caused if splitting generates some inconsistency in the boundary conditions for the ensuing subproblems. Therefore, it was decided to modify the non-homogeneous boundary fluxes at the injury site for factors IX/IXa, X/Xa, XI/XIa and tPA treating them as homogeneous boundary conditions with additional reaction terms only on the injury site for the coagulation factors listed above.

One of the main advantages of the operator splitting method is the possibility to choose different temporal discretization for each subproblem. Such a feature turns out to be particularly important in the case of stiff problems. Accordingly, we introduce two different time steps: Δt – for the diffusion subproblem and $\Delta s = \Delta t/10$ – for the reaction subproblem. With this approach, the diffusion term is computed only once and the reaction term is computed j times at each time step (in our case $j = 10$); then at each substep, only part of the reaction solution is updated. Both problems are discretized in space using the Galerkin approximation, based on the finite element method, and in time using first order implicit schemes.

The implementation is done with MATLAB in one-dimensional domain Ω_{1D} with the boundary $\partial\Omega_{1D}$ given by two points: in the center of the injury and on the opposite healthy blood vessel wall. Space and time discretization are chosen to be equal to $dx = 0.0005$ cm, $dt = 0.001$ min and $ds = 0.0001$

min.

We obtain the following solution that shows the evolution of all 23 chemical species in time on the injury site, see Figs. 1–3.

3.2 Initial conditions and unknown parameters for (27)

Before solving the synthetic model (1), an appropriate choice of initial conditions and unknown parameters for the virtual equation should be selected to make the solution agree with output of the benchmark model. We think that it is a reasonable way to obtain the required data, since the main body of the clot is built during the propagation phase while the foregoing phases are very short.

The initial conditions for the synthetic model (for factors I/Ia, II/IIa, ATIII, PC/APC, α_1AT, tPA, PLS/PLA and α_2AP) are provided by the solution of the benchmark model [1] at the end of the amplification phase, Table 3. The starting time of the synthetic model is conventionally identified with the time when fibrin has achieved its threshold equivalent to 350 nM. According to [20] this value corresponds to fibrin concentration when the first fibrin fibers appear. To obtain the prothrombinase initial concentration the following equation from the benchmark model was used

$$[W] = \frac{[Va] \cdot [Xa]}{K_{dW}}.$$

justified by the very high speed at which prothrombinase is produced in the presence of Va, Xa (and of activated platelets).

The unknown parameters k_w, h_{1W}, h_{2W} in the virtual equation (27) are selected according to the iterative process of simulations, trying to drive the solution of the synthetic model as close as possible to the solution of the

benchmark model, see Table 2. At this stage, the dimensionless platelets concentration C_P in (27) is taken to be equal to one and the blood flow impact is neglected since these features are absent in the benchmark model. In such a static framework, the further simplification of a one-dimensional growing clot can be considered.

3.3 Synthetic model: choice of parameters and resolution

We compute now the solution of the synthetic model that describes the blood coagulation process from the onset of the propagation phase in the one-dimensional domain Ω_{1D} to compare it with the benchmark model.

The computational domain Ω_{1D} is initially subdivided into two subregions: occluded Ω_{clot} and non-occluded $\Omega_{1D} \setminus \Omega_{clot}$ blood vessel parts. We say that production of active and consumption of non-active coagulation factors take place only in Ω_{clot} and in $\Omega_{1D} \setminus \Omega_{clot}$ the concentration of all chemical species stays as in the circulating blood.

Therefore, according to the synthetic model, it was assumed that the initial blood clot region $\Omega_{clot} = \{x \in \Omega_{1D} : -r \leq x \leq l^*\}$, where l^* represents the thickness of the initial clot, which we took equal to 10% of the vessel diameter[4], is initially present and fully included into the domain Ω_{1D}. The concentration of the chemical species inside Ω_{clot} is given as an output of the amplification phase and in $\Omega_{1D} \setminus \Omega_{clot}$ as the concentration in the circulating blood. Accordingly, the initial concentrations of active species (factors Ia, IIa, PLA, APC) and prothrombinase complex W are defined as smoothly decreasing functions from the initial concentrations inside Ω_{clot} to circulating blood concentration in $\Omega_{1D} \setminus \Omega_{clot}$. The same criterion is applied to the

[4]This choice is done consistently with the simulations of reaction-advection-diffusion problem coupled to the blood flow. When the initial clot is taken too small it becomes difficult to protect it from the wiping action blood flow.

non-active coagulation factors: they are defined as smoothly increasing functions from the initial concentration values inside Ω_{clot} up to the fresh blood concentration in $\Omega_{1D} \setminus \Omega_{clot}$.

The numerical resolution of the synthetic model in the one-dimensional case is done in the same manner as for the benchmark model: a first-order operator splitting method is applied to decouple the diffusion part from the reaction part to solve them sequentially. Both subproblems are solved using the Euler implicit time discretization scheme on a time interval $T \supset \hat{T} = [t_{PP}, T]$, where $t_{PP} = 1.91$ min $> t_0$ corresponds to the time moment when the propagation phase (PP) has started and fibrin has achieved its threshold. We use time step and space discretization identical to the benchmark model: $\Delta t = 0.001$ min, $\Delta s = 0.0001$ min and $\Delta x = 0.0005$.

As a result, we obtain the numerical solution of the synthetic model in the one-dimensional case, represented in Figs. 4 and 5. We point out that the process does not start from the time $t = 0$, but from t_{PP}.

The comparison between the benchmark and synthetic models for thrombin and fibrin is shown in Fig. 6. It can be seen that the solution for fibrin concentration obtained for the synthetic model matches almost perfectly the solution of the benchmark model. The comparison is almost equally good for thrombin.

The computational advantage of working with much less differential equations is very concrete, since it allows to deal more easily with the complicated geometries usually characterizing the real biological process. In this spirit, we proceed with the analysis of the reduced model in the two-dimensional case including the action of the blood flow on the biochemical cascade.

4 Blood slip impact

In this section the numerical solution of the synthetic model is discussed where the blood slip velocity impact on the concentration of activated platelets is taken into account. For simplicity we confine to the two-dimensional case. The obtained results are compared with the case of no-slip velocity for which the dimensionless concentration of activated platelets was taken to be equal to one.

For blood flow a generalised Newtonian model with the shear-thinning Cross rheological model [12] is chosen and Navier's slip boundary conditions are adopted in such a way that no-penetration condition is imposed in the normal direction and a non-zero tangential velocity is considered along the blood vessel walls[5]. The dimensionless platelets concentration in (27) is then computed according to (40). We stress that when evaluating the coefficient H in (40) in the two-dimensional case the length H coincides with the lesion width (the lesion is normal to the flow).

The numerical simulations of the platelets-fibrin clot evolution starting from the onset of the propagation phase up to total dissolution have been performed using the open source finite element solver FreeFem++ and are presented in Fig. 7. Several snapshots associated to different phases of clot formation are shown to indicate the fibrin concentration profiles and the streamlines of the blood flow.

The evolution of concentration of thrombin and fibrin in this case is compared to the case of no-slip velocity and is shown in Fig. 8. From these graphs one can see that platelets supplied by the blood slip velocity to the clotting region do really play an important role in the clot formation. In particular, two specific aspects can be distinguished: the amount of produced

[5]Details regarding the slip velocity magnitude are given in [21, 22].

chemical species increases significantly and the thrombin burst occurs earlier in case of higher platelets provision to the clotting site.

5 Conclusions

The synthetic blood coagulation model has been solved in the one-dimensional case (with stagnating blood), using as initial condition the output of the amplification phase given by the benchmark model. The obtained solution was compared with the solution of the benchmark model, in order to choose the appropriate coefficients for the prothrombinase dynamics in the synthetic model. Then, passing to situations closer to the natural process, it has been shown that this much simpler model can stand as an acceptable alternative to the benchmark model, allowing to deal more easily with the complex geometry and flows typical of coagulation processes.

The choice of initial conditions for the synthetic model and of the unknown parameters for the virtual equation was discussed at length.

The synthetic model was used to study the influence of the blood flow and the contribution of slip velocity on the dimensionless platelets concentration. The solution was compared with the one obtained for the no-slip velocity case, and it was observed that the slip velocity may have a significant impact on the evolution of the whole process.

The extension of these results to the three-dimensional case presents additional modeling and computational challenges and will be carried out in a forthcoming paper.

Acknowledgments

This work was supported by Fundação para a Ciência e a Tecnologia (FCT) through the grant SFRH/BD/63334/2009 and the Center for Mathematics and its Applications of the Instituto Superior Técnico, University of Lisbon, in particular the project PHYSIOMATH (EXCL/MAT-NAN/0114/2012). The authors would like to thank Simone Rossi for meaningful discussions and valuable suggestions.

References

[1] M. Anand, K. Rajagopal and K.R. Rajagopal, A model for the formation, growth, and lysis of clots in quiescent plasma. A comparison between the effects of antithrombin III deficiency and protein C deficiency, *Journal of Theoretical Biology* **253** (2008), 725–738.

[2] S.T. Appiah, I.A. Adetunde and I.K. Dontwi, Mathematical model of blood clot in the human cardiovascular system, *International Journal of Research in Biochemistry and Biophysics* **1**(2) (2011), 9–16.

[3] F.I. Ataullakhanov, G.T. Guria, V.I. Sarbash and R.I. Volkova, Spatiotemporal dynamics of clotting and pattern formation in human blood, *Biochimica et Biophysica Acta* **1425** (1998), 453–468.

[4] F.I. Ataullakhanov and M.A. Panteleev, Mathematical modeling and computer simulation in blood coagulation, *Pathophysiol Haemost Thromb* **34** (2005), 60–70.

[5] R.C. Becker, Cell-based models of coagulation: a paradigm in evolution, *Journal of Thrombosis and Thrombolysis* **20**(1) (2005), 65–68.

[6] T. Bodnár and A. Sequeira, Numerical simulation of the coagulation dynamics of blood,*Computational and Mathematical Methods in Medicine* **9**(2) (2008), 83–104.

[7] I. Borsi, A. Farina, A. Fasano and K.R. Rajagopal, Modelling the combined chemical and mechanical action for blood clotting. In: *Nonlinear Phenomena with Energy Dissipation, Gakuto Internat Ser Math Sci Appl*, Gakkotosho, Tokyo, **29** (2008), 53–72.

[8] A. Fasano, J. Pavlova and A. Sequeira, A synthetic model for blood coagulation including blood slip at vessel wall, *Clinical Hemorheology and Microcirculation* **51** (2012), 1–14.

[9] A. Fasano, R. Santos and A. Sequeira, Blood coagulation: a puzzle for biologists, a maze for mathematicians. In *Modelling Physiological Flows*, D. Ambrosi, A. Quarteroni, G. Rozza (Editors), Springer Italia Chapt. 3, (2011) 44-77, DOI 10.1007/978-88-470-1935-53.

[10] A.L. Fogelson and J.P. Keener, Toward an understanding of fibrin branching structure, *Phys Rev E Stat Nonlin Soft Matter Phys* **81**(5–1) (2010), 051922.

[11] A.I. Fogelson and R.D. Guy, Immersed-boundary-type models of intravascular platelet aggregation, *Comput Appl. Mech. Engrg.* **197** (2008), 2087–2104.

[12] A.M Gambaruto, J. Janela, A. Moura and A. Sequeira, Sensitivity of hemodynamics in a patient specific cerebral aneurysm to vascular geometry and blood rheology, *Mathematical Biosciences and Engineering* **8**(2) (2011), 409–423.

[13] M. Hoffman, Remodeling the blood coagulation cascade, *Journal of Thrombosis and Thrombolysis* **16**(1/2) (2003), 17–20.

[14] M. Hoffman, A cell-based model of coagulation and the role of factor VIIa, *Blood Reviews* **17** (2003), 51–55.

[15] T. Jahnke and C. Lubich, Error bounds for exponential operator splittings, *BIT*, **40**(4) (2000), 735–744.

[16] D. Lanser and J.G. Verwer, Analysis of operator splitting for advection-diffusion-reaction problems from air pollution modelling, *Journal of Computational and Applied Mathematics* **111** (1999), 201–216.

[17] K. Leiderman and A.L. Fogelson, Grow with the flow: a spatial–temporal model of platelet deposition and blood coagulation under flow, *Mathematical Medicine and Biology* **28** (2011), 47–84.

[18] R.I. McLachlan and G.R.W. Quispel, Splitting methods, *Acta Numerica* **11** (2002), 341–434.

[19] G. Moiseyev, S. Givli and P.Z. Bar-Yoseph, Fibrin polymerization in blood coagulation–A statistical model, *Journal of Biomechanics* **46** (2013), 26–30.

[20] M.V. Ovanesov, N.M. Ananyeva, M.A. Panteleev, F.I. Ataullakhanov and E.L. Saenko, Initiation and propagation of coagulation from tissue factor-bearing cell monolayers to plasma: initiator cells do not regulate spatial growth rate, *J Thromb Haemost* **3** (2005), 321–331.

in their binding of the components of the intrinsic factor X-activating complex, *J Thromb Haemost* **3** (2005), 2545–2553. *PNAS* **103**(46) (2006), 17164–17169.

[21] J. Pavlova, A. Fasano, A. Sequeira, Numerical simulations of a reduced model for blood coagulation (Submitted).

[22] J. Pavlova, Mathematical modelling and numerical simulations of blood coagulation, PhD Thesis, Lisbon University, 2014.

[23] B. Sportisse, An analysis of operator splitting techniques in the stiff case, *Journal of Computational Physics* **161** (2000), 140–168.

[24] P.P. Tanos, G.K. Isbister, D.G. Lalloo, C.M.J. Kirkpatrick and S.B. Duffull, A model for venom-induced consumptive coagulopathy in snake bite, *Toxicon* **52** (2008), 769–780.

[25] F.F. Weller, A free boundary problem modeling thrombus growth: Model development and numerical simulation using the level set method, *J Math Biol* **61**(6) (2010), 805–818.

[26] M.F. Wheeler and C.N. Dawson, An operator-splitting method for advection-diffusion-reaction problem, Technical Report 87-9, Rice University, Houston, Texas, 1987.

[27] S. Zhao, J. Ovadia, X. Liu, Y.-T. Zhang and Q. Nie, Operator splitting implicit integration factor methods for stiff reaction-diffusion-advection systems, *J Comput Phys* **230**(15) (2011), 5996–6009.

Table 1: Boundary conditions for the benchmark model [1].

Coag. factors	**Boundary flux terms B_i**	**Coag. factors**	**Boundary flux terms B_i**
IXa	$\frac{k_{7,9}[IX][TF-VIIa]}{K_{7,9M}+[IX]}\frac{L}{D_{IXa}}$	IX	$-\frac{k_{7,9}[IX][TF-VIIa]}{K_{7,9M}+[IX]}\frac{L}{D_{IX}}$
Xa	$\frac{k_{7,10}[X][TF-VIIa]}{K_{7,10M}+[X]}\frac{L}{D_{Xa}}$	X	$-\frac{k_{7,10}[X][TF-VIIa]}{K_{7,10M}+[X]}\frac{L}{D_{X}}$
XIa	$\frac{\phi_{11}[XI][XIIa]}{\Phi_{11M}+[XI]}\frac{L}{D_{XIa}}$	XI	$-\frac{\phi_{11}[XI][XIIa]}{\Phi_{11M}+[XI]}\frac{L}{D_{XI}}$
tPa	$\left(k^C_{tPA}+k^{IIa}_{tPa}+k^{Ia}_{tPA}\right)\frac{[ENDO]L}{D_{tPA}}$		

* According to [1] parameter L represents the thickness of the plasma layer that covers the thrombogenic plane and $[ENDO]$ stands for the surface density of the endothelial cells that secrete tPA.

Table 2: Reaction rates and kinetic constants [1]

Coagulation factors	**Parameters**
W	$k_W = 160$ min^{-1}
W/APC	$h_{1W} = 2.2 \times 10^{-3}$ nM^{-1} min^{-1}
W/ATIII	$h_{2W} = 1 \times 10^{-2}$ nM^{-1} min^{-1}
II/IIa	$k_2 = 1344$ min^{-1}, $K_{2M} = 1060$ nM
IIa/ATII	$h_2 = 0.714$ nM^{-1} min^{-1}
I/Ia	$k_1 = 3540$ min^{-1}, $K_{1M} = 3160$ nM
Ia	$h_1 = 1500$ min^{-1}, $H_{1M} = 250000$ nM
PC/APC	$k_PC = 39$ min^{-1}, $K_{PCM} = 3190$ nM
APC/α_1AT	$h_{APC} = 6.6 \times 10^{-7}$ nM^{-1} min^{-1}
PLS/PLA	$k_{PLA} = 12$ min^{-1}, $K_{PLAM} = 18$ nM
PLA/α_2AP	$h_{PLA} = 0.096$ nM^{-1} min^{-1}

Table 3: Initial conditions for the reduced model [1, 21, 22].

Coagulation factors	**Initial clot concentration (nM)**	**Circulating blood concentration (nM)**
W	1.0843	0.0*
II	1195.8306	1400.0
IIa	0.6865	0.0*
I	6654.5100	7000.0
Ia	350.1488	0.0*
PC	59.8972	60.0
APC	0.1588	0.0*
ATIII	1566.1334	3400.0
α_1AT	44999.8284	45000.0
PLS	2178.26097	2180.0
PLA	3.8671	0.0*
α_2AP	104.9480	105.0
tPA	0.0906	0.08

* Concentration of activated coagulation factors in the circulated blood for the numerical simulation is taken to be equal to 0.01% of the corresponding non-active coagulation factors.

Figures

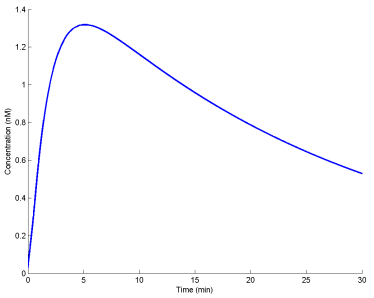

(a) Factor XIa concentration

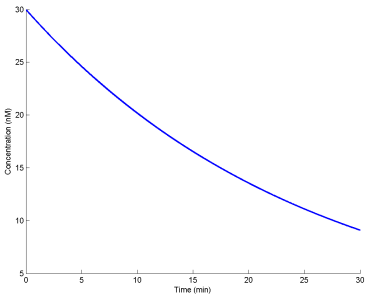

(b) Factor XI concentration

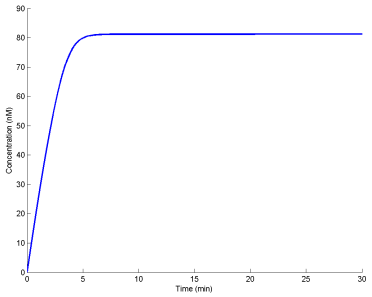

(c) Factor IXa concentration

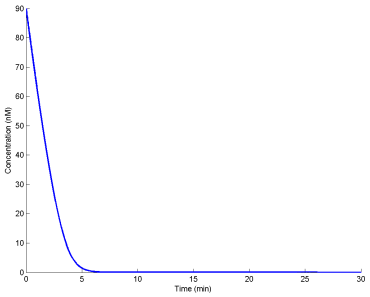

(d) Factor IX concentration

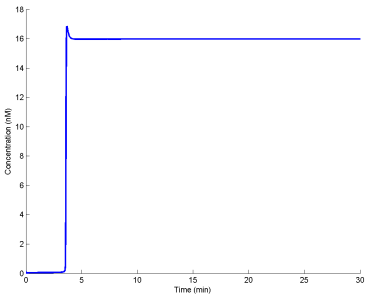

(e) Factor Xa concentration

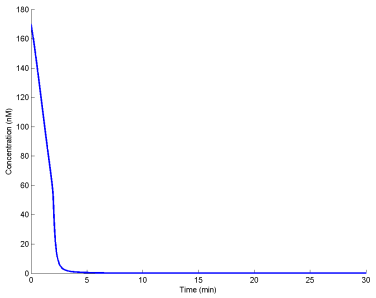

(f) Factor X concentration

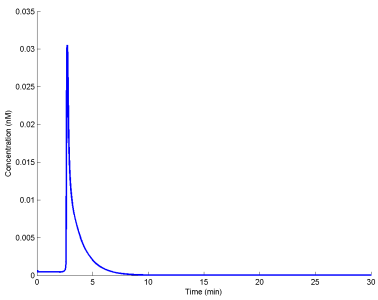

(g) Factor VIIIa concentration

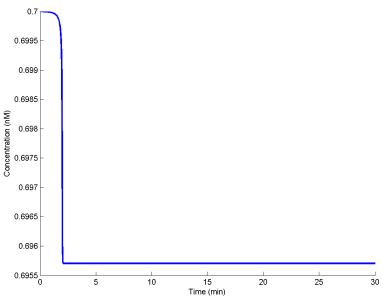

(h) Factor VIII concentration

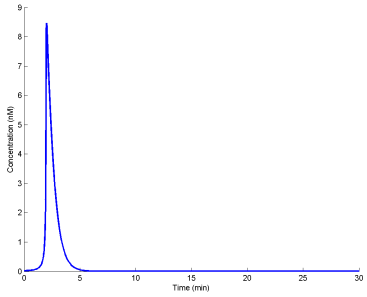

(a) Factor Va concentration

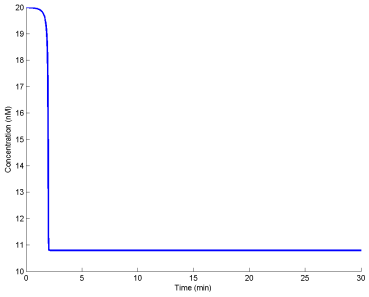

(b) Factor V concentration

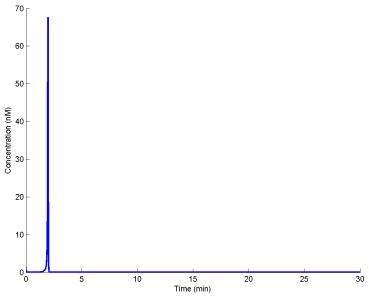

(c) Thrombin concentration

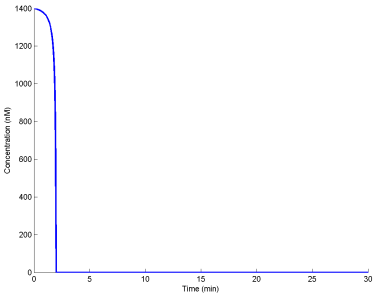

(d) Prothrombin concentration

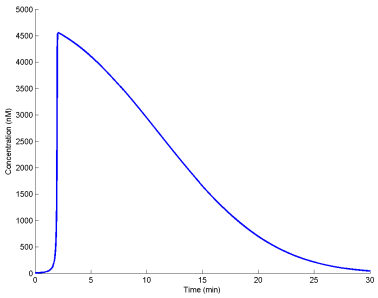

(e) Fibrin concentration

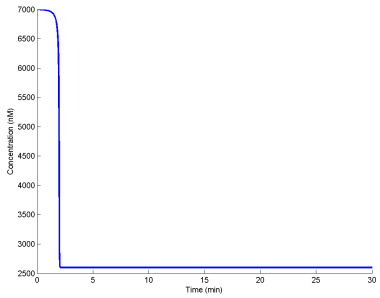

(f) Fibrinogen concentration

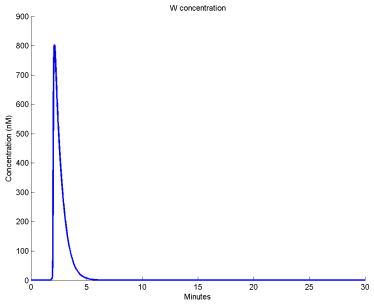

(g) Prothrombinase concentration

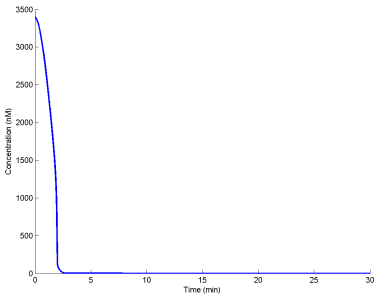

(h) ATIII concentration

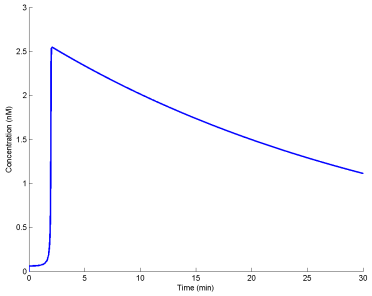

(a) APC concentration

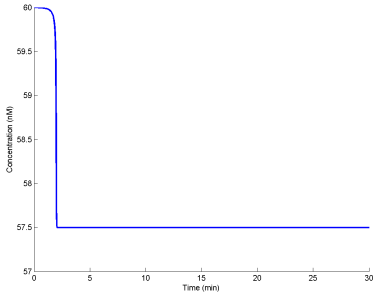

(b) PC concentration

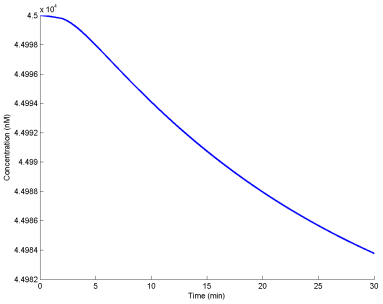

(c) α_1AT concentration

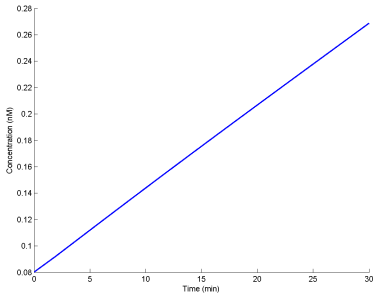

(d) tPA concentration

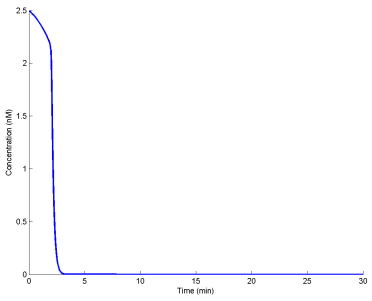

(e) Tissue Factor Pathway Inhibitor concentration

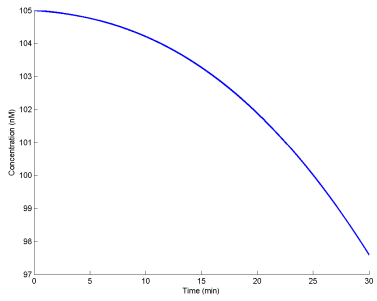

(f) α_2AP concentration

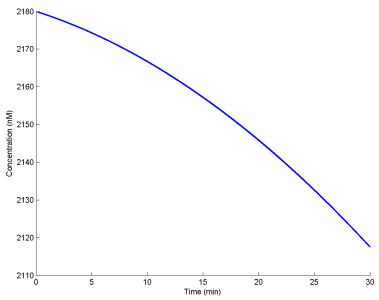

(g) PLS concentration

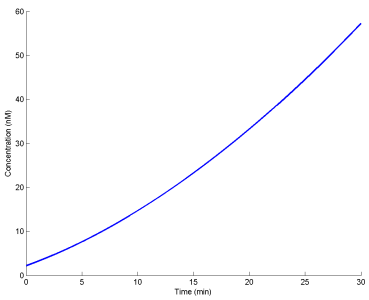

(h) PLA concentration

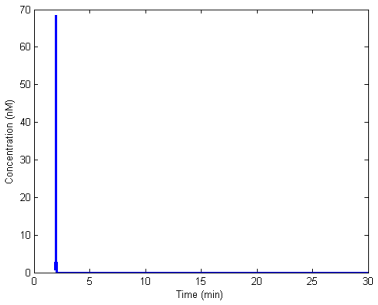

(a) Thrombin concentration

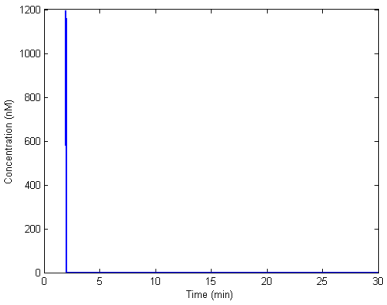

(b) Prothrombin concentration

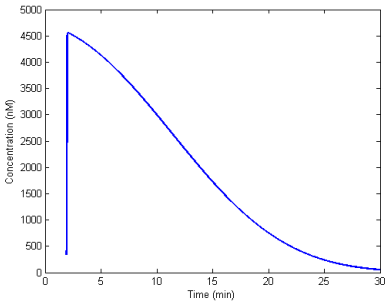

(c) Fibrin concentration

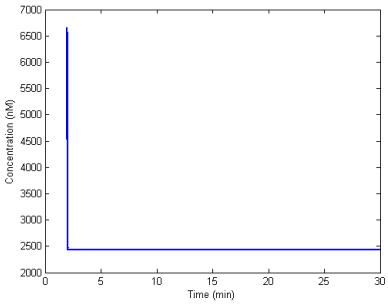

(d) Fibrinogen concentration

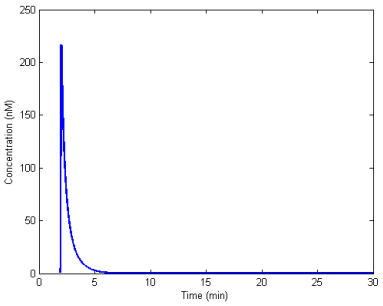

(e) Prothrombinase concentration

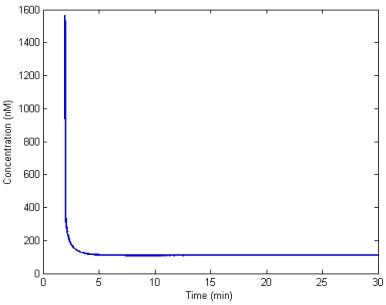

(f) ATIII concentration

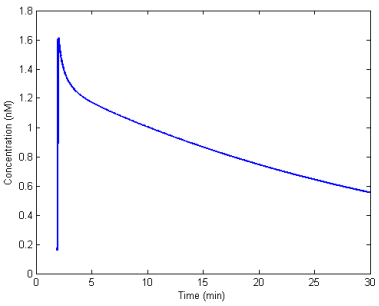

(g) APC concentration

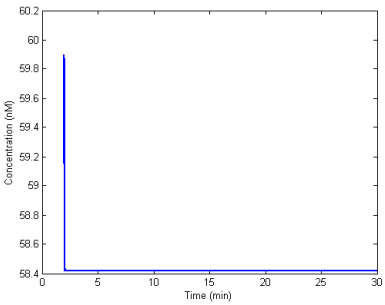

(h) PC concentration

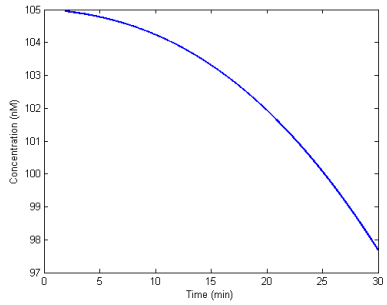

(a) α_2AP concentration

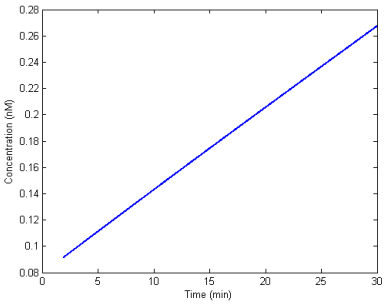

(b) tPA concentration

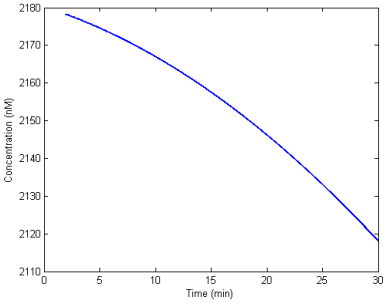

(c) PLS concentration

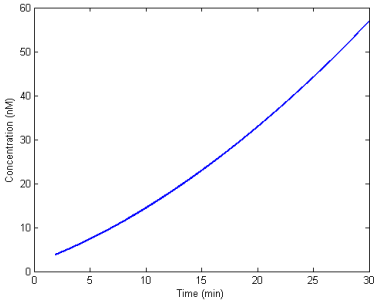

(d) PLA concentration

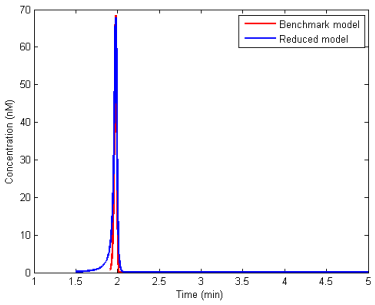

(a) Thrombin concentration

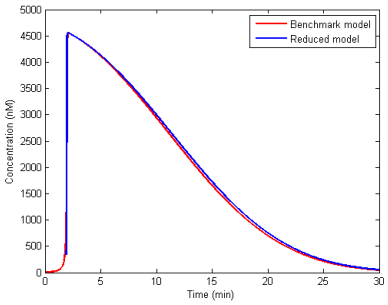

(b) Fibrin concentration

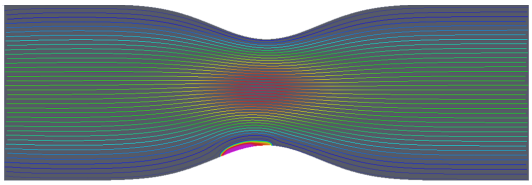

(a) Onset of the propagation phase

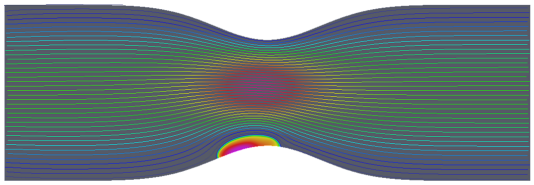

(b) Propagation phase (I)

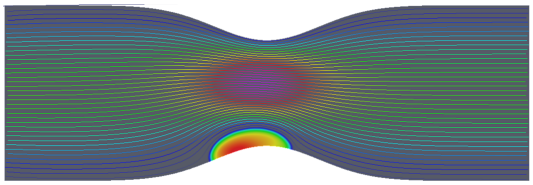

(c) Propagation phase (II)

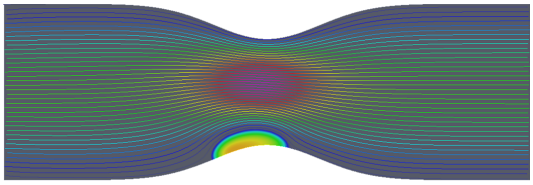

(d) Fibrinolysis (I)

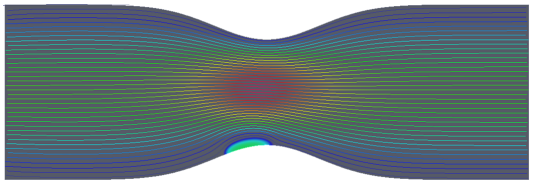

(e) Fibrinolysis (II)

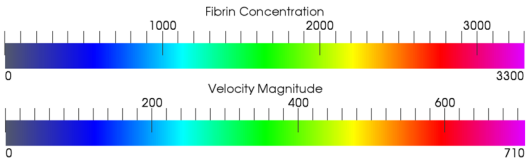

(f) Scale of fibrin concentration

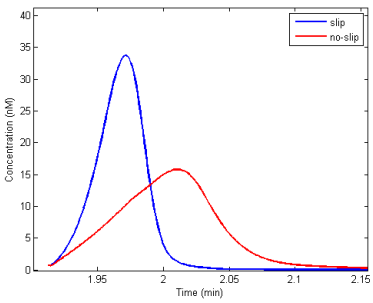

(a) Thrombin concentration

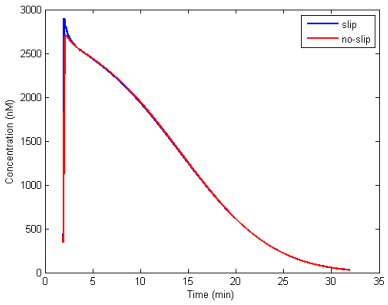

(b) Fibrin concentration

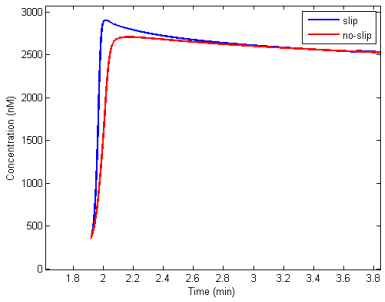

(c) Zoom of fibrin concentration